

1
2
3
4
5
6
7
8
9
10
11
12
13
14
15
16
17
18
19
20
21
22
23
24
25
26
27

Research Article

The Kishony Mega-Plate Experiment, a Markov Process

Short Title: The Kishony Mega-Plate Experiment

Corresponding Author:

Alan Kleinman

PO Box 1240

Coarsegold, CA 93614 USA

Tel: (559) 642-4105

E-mail: kleinman@sti.net

Number of Tables: 0

Number of Figures: 11

Word count: 8764

Keywords:

1. Drug-resistance
2. Evolution
3. Markov Process
4. Kishony Mega-Plate experiment
5. Infectious Diseases

28 **Abstract**

29 A correct understanding of the DNA evolution of drug resistance is critical in developing
30 strategies for suppressing and preventing this process. The Kishony Mega-Plate Experiment
31 demonstrates this important phenomenon that occurs in the practice of medicine, that of the
32 evolution of drug-resistance. The evolutionary process which the bacteria in this experiment are
33 doing is called a Markov Process or Markov Chain. Understanding this process enables clinicians
34 and researchers to predict the evolution of drug-resistance and develop strategies to prevent
35 this process. This paper will show how to apply the Markov Chain model of DNA evolution to the
36 Kishony Mega-Plate Experiment and why the experiment behaves the way it does by contrasting
37 the Jukes-Cantor model of DNA evolution (a stationary model) with a modification of the Jukes-
38 Cantor model that makes it a non-stationary, non-equilibrium Markov Chain. The numerical
39 behaviors of the stationary and non-stationary models are compared. What this analysis shows
40 is that DNA evolution is a non-stationary, non-equilibrium process and that by using the correct
41 non-stationary, non-equilibrium model that one can simulate and predict the behavior of real
42 evolutionary examples and that these analytical tools can give the clinician guidance on how to
43 use antimicrobial selection pressures for treating infectious diseases. This in turn can help
44 reduce the numbers and costs of hospitalization for sepsis, pneumonia and other infectious
45 diseases.

46 **Introduction**

47 The Kishony Mega-Plate Experiment is described in the paper “Spatiotemporal microbial
48 evolution on antibiotic landscapes” [1]. A description of how to make a Mega-Plate Experiment
49 can be found in reference [2]. Many videos of the experiment can be found on the internet, a
50 good example can be found here [3]. The next paragraph gives a simple explanation of the
51 experiment.

52

53 The experiment consists of the following. A large petri dish is constructed. Growth media is
54 placed on this petri dish, and in this growth media, different concentrations of an antimicrobial
55 agent are placed in bands in the growth media. In the left and right-hand bands in the petri dish,
56 no antimicrobial agent is used. In the next adjacent bands to these zero concentration bands, the
57 lowest concentration of the drug is used. As one move to the center of the petri dish, increasing
58 concentrations of the drug are placed in each band until in the middle of the dish that contains
59 the highest concentration of the antimicrobial agent. Then a motile “wild-type” bacteria
60 (founder) is introduced into the petri dish that has no resistance initially to the antimicrobial
61 agent used and is only able to grow in the drug-free region. As these colonies in the drug-free
62 regions grow, mutations occur in some members of these colonies. Occasionally, some member
63 gets a beneficial mutation that enables it to grow in the next higher drug-concentration region.
64 That new variant with the first resistance mutation now forms a new colony that can grow in the
65 lowest drug concentration region. As that new colony grows, one of its members gets another
66 beneficial mutation that allows it to grow in the next higher drug-concentration region. This
67 process continues until finally there is a variant that can grow in the high drug-concentration
68 region.

69

70 For this experiment to work in this size petri dish, the increase in concentration for adjacent
71 bands must be limited so that it only requires a single beneficial mutation to occur on some
72 member of the drug-sensitive variant population in the next lower drug-concentration band to
73 grow in the next higher drug-concentration band. As the population increases in a particular
74 band, descendants are getting mutations in their DNA as replications occur. This is a random
75 walk process where the number of members taking their particular random walk increases as
76 the population grows in number and as different variants occur. Some variants on their own
77 particular random walk accumulate particular mutations that give improved fitness to the
78 antibiotic selection pressure allowing these variants to grow in the higher drug-concentration
79 regions. This process can be mathematically modeled as a Markov Process. A variety of different
80 Markov Models of DNA evolution have been proposed. One of the earliest models is the Jukes-
81 Cantor model presented in 1969 [4]. Many derivative models have been proposed such as the
82 K80 [5] and K81 [6] (1980 and 1981 Kimura models respectively), the F81 Felsenstein model [7]
83 presented in 1981, HKY85 model [8] (Hasegawa, Kishino and Yano 1985) model, the T92 model
84 [9] (Tamura 1992), and the TN93 model [10] (Tamura and Nei 1993). The Jukes-Cantor and
85 derivative models are commonly used in an attempt to compute the evolutionary distance
86 between different sequences of homologous genetic code. Some recent examples of applications
87 of the Jukes-Cantor and derivative models can be found in the following references, [11-15]. The
88 main difference between the Jukes-Cantor model and the derivative models listed above is
89 derivative models allow for different mutation rates for the different elements of the transition

90 matrix, for example, to address the fact that base transversions can have a different mutation
91 rate than for base transitions. However, the transition matrix is still constant over time.

92

93 Huelsenbeck and his co-authors wrote: "At present, a universal assumption of model-based
94 methods of phylogenetic inference is that character change occurs according to a continuous-
95 time Markov chain. At the heart of any continuous-time Markov chain is a matrix of rates,
96 specifying the rate of change from one character state to another. For many phylogenetic
97 analyses using DNA sequence data, it is assumed that there are four states (the nucleotides A, C,
98 G, T/U) with a 4 x 4 matrix of rates among the 12 possible nucleotide substitutions. A few
99 standard models of DNA substitution have been proposed. These include those first described by
100 Jukes and Cantor (1969), Kimura (1980, 1981), Felsenstein (1981, 1984), Hasegawa, Yano, and
101 Kishino (1984, 1985), Tamura and Nei (1993), and Tavare' (1986)."[16] The intention here in
102 this paper is to give a proposed modification of the heart of the Markov chain model that is
103 demonstrated to correlate with the experimental model, the Kishony Mega-Plate experiment.

104

105 The Jukes-Cantor and derivative models listed above have a property in common. These models
106 assume that the elements of the Markov transition matrix are constant with each replication. It
107 is shown this implicit assumption gives a model constrained to constant population size, and
108 that constant population size is 1. This assumption gives a model that fails to correctly model the
109 evolution of antimicrobial resistance. A modification of the Jukes-Cantor model is presented that
110 allows for modeling DNA evolution in different population sizes and that the population can vary
111 at each evolutionary transitional step (replication). The mathematics for these two Markov
112 models are described in the next section. The results are compared and the Markov model which
113 takes into account population size is shown to compare favorably with the experimental results
114 of the Kishony Mega-Plate experiment.

115 **Materials and Methods**

116 **Statistical Analysis**

117 The statistical analysis used in this study is based on the Markov process. A Markov process is a
118 stochastic or random process where future outcomes can be predicted based solely on the
119 present state of the system. A Markov process for discrete events is called a Markov chain. When
120 formulated correctly, a Markov chain that models DNA evolution gives the theoretical
121 distribution of frequencies of the different variants in a growing population based on the
122 population size, the mutation rate, and the known initial state of the population. The formulation
123 of such a model consists of the following steps.

124

125 The first step is to identify the possible states in which the system can be. When modeling DNA
126 evolution, a given site in a genome can be in one of four possible states (one of the four possible
127 DNA bases). When considering two sites simultaneously in a genome, those two sites can be in
128 16 possible states (4^2 possible combinations of bases). When considering three sites, the number
129 of possible states for the system is 64 possible states (4^3 possible combinations). As one
130 considers more sites in the genome, the number of possible states goes up exponentially. Once
131 the number of sites that are to be considered is determined, the number of possible states for

132 each of those sites and the number of transitions between one state and another needs to be
133 determined when a replication of those sites occur.

134

135 When DNA is replicated, it is not a perfect process, occasionally errors occur. The frequency of
136 error can be based on a single replication, and for this analysis, that is how the mutation rate is
137 considered. Upon replication, the base at a given site can be replicated with fidelity giving the
138 same base as the original copy, or the base can be replicated incorrectly and replaced with a
139 different base, a mutation has occurred. Each of those possible transitions on replication has a
140 probability associated with that transition. When considering a single-site DNA evolutionary
141 process, each state will have four possible transitions, and since a single-site DNA evolutionary
142 process has four possible states, it will have 16 (4^2) possible transitions. When considering a
143 two-site DNA evolutionary process, the 16 possible states will have 256 (16^2) possible
144 transitions. And when considering the three-site DNA evolutionary process, the 64 possible
145 states will have 4096 (64^2) possible transitions. Once the number of sites in the genome is
146 determined to be analyzed, the number of states and state transitions can be determined, and
147 the states and transitions can be organized into matrices. The state matrix is a 1 x number of
148 states matrix where the elements of this matrix are the frequencies of each of the possible states
149 of the system at a particular time. The matrix of transitions will be a square dimension equal to
150 the number of possible states where each element of this matrix is the probability of transition
151 from one state to another possible state. These transition probabilities depend on the mutation
152 rate but also depend on the population size. If one assumes that the population size remains
153 constant, the transition matrix will remain constant over time and, a “stationary” transition
154 matrix is obtained and, the transition probabilities remain constant over time. However, if the
155 population size is changing over time, a “non-stationary” transition matrix is obtained and, the
156 transition probabilities will change over time as the population size changes. This is
157 demonstrated by the derivation of the one and two-site DNA evolutionary models for a
158 stationary Markov chain (the Jukes-Cantor model) and the non-stationary variable population
159 model. The evaluation of these Markov chains over time to obtain the frequencies of the
160 different states after each replication is done by simple matrix multiplication.

161 The Markov Process

162 A Markov chain is a stochastic or random mathematical model describing a sequence of possible
163 events where each event depends only on the state attained in the previous event. Continuous-
164 time Markov chains are called Markov processes and are named after the Russian
165 mathematician Andrey Markov [17]. The relationship between this mathematics and the
166 Kishony Mega-Plate experiment is that with every replication of the bacteria, the offspring
167 potentially get a random mutation that in some cases will allow that variant to make a transition
168 and grow in the next higher drug-concentration region. A well known Markov model of DNA
169 evolution is the Jukes-Cantor Markov Chain model of DNA evolution.[4] There are many
170 derivative models based on the Jukes-Cantor model but none of these models correctly describe
171 the Kishony Mega-Plate experiment. The reason is that the Jukes-Cantor model is based on a
172 stationary transition matrix that gives a Markov process that rapidly reaches equilibrium. The
173 DNA evolutionary process is a highly non-stationary process which does not readily reach
174 equilibrium. An alternative non-stationary transition matrix based on a small modification of the
175 Jukes-Cantor model is presented and the results contrasted with the Jukes-Cantor model.

176 The State Transition Markov Model for a single-site in a Genome

177 DNA evolution can be mathematically modeled as a discrete Markov Chain. The way this is done
 178 for the Kishony Mega-Plate Experiment is as follows. E_1, E_2, E_3, \dots are the states of the Markov
 179 Chain. The way to understand these states for this experiment, consider the first evolutionary
 180 step. The wild type bacteria do not have any variants with a mutation which would give them
 181 some resistance to the drug these bacteria are challenged. Some site in the bacterial genome
 182 lacks the correct DNA base at that site. Replication of a bacterium is the random trial at each
 183 transitional step of this Markov process. There are four possible bases for that site, adenine (A),
 184 guanine (G), cytosine (C), and thymine (T). Each of those possible bases represents a Markov
 185 state. Figure 1 is a diagram of the possible state transitions for this Markov process. The letter μ
 186 is the mutation rate that is assumed constant for each of the possible transitions. The state
 187 transition diagram for this Markov process is illustrated in Figure 1.

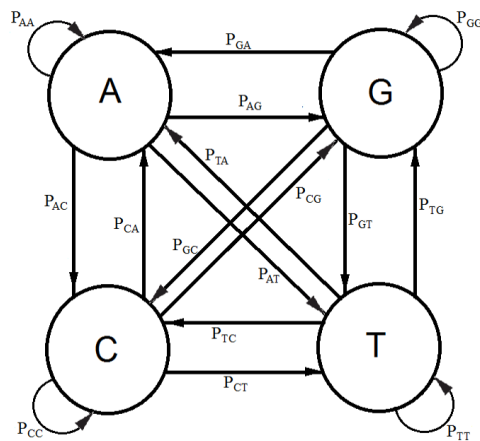


Illustration 1: State Transition Diagram for a single mutation at a particular site in the genome.

188 When replication of the bacterium occurs, if the base at the particular site is T, its descendant
 189 can get a T at that site, no mutation occurs, or an A, C, or G base can occur at that site, a mutation
 190 occurs. If the base at that site is not a T (that is A, C, or G), then any of the possible bases at that
 191 site can be mutated to give a T for that descendant at that particular site. A transition matrix that
 192 describes the evolutionary change in time t is:

$$P(t) = \begin{pmatrix} p_{AA} & p_{AC} & p_{AG} & p_{AT} \\ p_{CA} & p_{CC} & p_{CG} & p_{CT} \\ p_{GA} & p_{GC} & p_{GG} & p_{GT} \\ p_{TA} & p_{TC} & p_{TG} & p_{TT} \end{pmatrix}$$

193

(1)

194 $P = (p_{ij})$ where the p_{ij} gives the probabilities of change from the state E_i to E_{i+1} at time $t + \Delta t$ where
195 Δt is a replication (for the Jukes-Cantor stationary model, it is also a generation). If insertions,
196 deletions, transpositions, and other types of mutations are neglected (that is substitutions only),
197 the transition matrix would look as follows:

$$P = \begin{pmatrix} 1-\mu & \mu/3 & \mu/3 & \mu/3 \\ \mu/3 & 1-\mu & \mu/3 & \mu/3 \\ \mu/3 & \mu/3 & 1-\mu & \mu/3 \\ \mu/3 & \mu/3 & \mu/3 & 1-\mu \end{pmatrix} \quad (2)$$

199 The subscripts on p represent each of the possible transitions. For example, an AA subscript
200 means on replication, the adenine base was replicated by another adenine base, no mutation
201 occurs. A CG subscript means that on replication a cytosine base was replaced by a guanine base
202 (a mutation has occurred) and so on. Based on the assumption that the mutation rates are
203 constant, the p_{ij} elements in terms of the mutation rate can be written as follows and gives the
204 Jukes-Cantor stationary model:

205 Implicit in the Jukes-Cantor model is the assumption that only a single member of the population
206 is considered. That bacterium replicates, and the Jukes-Cantor model is correct for that first
207 replication. However, for the next replication there are two members of the population, and
208 because of that increase in population size, the change in the relative frequency of the variants
209 must decrease, and that decrease in probabilities for a transition to a different base will not
210 follow the pattern presented by the Jukes-Cantor model. The distribution of variants for the
211 single drug is written as:

$$212 \quad n_A/n + n_C/n + n_G/n + n_T/n = 1 \quad (3)$$

213 Where n_A , n_C , n_G , and n_T are the number of members (replications) with the A, C, G, and T base at
214 the particular site in the population respectively, and n is the total number of members
215 (replications) in the population. For example, if A is assumed to be the variant with the
216 beneficial mutation for the drug and the initial wild-type bacterium has T at that site, then,
217 initially, n_A , n_C , and n_G , are 0, and n_T and n are 1. However, with the first replication, there is a
218 small probability that n_A , n_C , or n_G , is 1, a much higher probability that n_T is 2, and n will be 2.
219 With each additional replication, there will be a small probability that n_A , n_C , or n_G , will increase
220 by 1, but a much higher probability that n_T will increase by 1, and n will increase by 1. With each
221 additional replication, the frequencies of the A, C, and G variants will slowly increase while the
222 frequency of the T variant will very slowly decrease. This effect is not taken into account in the
223 standard Jukes-Cantor stationary model. The probabilities for a variable population model is
224 written:

$$225 \quad p_{ij} = \mu/(3*n), \quad i \neq j \quad \text{where } n=1,2,3,\dots \quad (4)$$

226 n is the total number of replications (the total population size) in the colony of bacteria. The
 227 expected number of members with the mutation A is $n_A=A*n$ where A is the frequency of the A
 228 variant after the population has done n replications and so on for the other possible variants.
 229 And the corresponding non-stationary Jukes-Cantor transition matrix becomes:

$$230 \quad P = \begin{pmatrix} 1-\mu/n & \mu/(3*n) & \mu/(3*n) & \mu/(3*n) \\ \mu/(3*n) & 1-\mu/n & \mu/(3*n) & \mu/(3*n) \\ \mu/(3*n) & \mu/(3*n) & 1-\mu/n & \mu/(3*n) \\ \mu/(3*n) & \mu/(3*n) & \mu/(3*n) & 1-\mu/n \end{pmatrix} \quad (5)$$

231 The initial state for either the stationary Jukes-Cantor model or the non-stationary Jukes-Cantor
 232 model is written:

$$233 \quad E_0 = (A_0, C_0, G_0, T_0) \quad (6)$$

234 Where the A_0, C_0, G_0, T_0 terms are the frequencies of the particular variant in the initial state.
 235 (When $A, C, G,$ or T are italicized indicates the frequencies for the particular variants with that
 236 base at that site.) And the state of the system at the time t_i is:

$$237 \quad E_i = (A_i, C_i, G_i, T_i) \quad (7)$$

238 At time t_i , the Markov Chain is in state E_i , then the state of the system at time $t_i + \Delta t$, where Δt is
 239 one replication, it will be in state E_{i+1} depends only on i , and t . The state of the system at time t_{i+1}
 240 is computed by doing the matrix multiplication using the following equation:

$$241 \quad E_{i+1} = E_i P \quad (8)$$

242 The matrix multiplication for the Jukes-Cantor model is:

$$243 \quad (A_{i+1}, C_{i+1}, G_{i+1}, T_{i+1}) = (A_i, C_i, G_i, T_i) \begin{pmatrix} 1-\mu & \mu/3 & \mu/3 & \mu/3 \\ \mu/3 & 1-\mu & \mu/3 & \mu/3 \\ \mu/3 & \mu/3 & 1-\mu & \mu/3 \\ \mu/3 & \mu/3 & \mu/3 & 1-\mu \end{pmatrix} \quad (9)$$

244 And the matrix multiplication for the non-stationary version of the Jukes-Cantor model
 245 is:

$$246 \quad (A_{i+1}, C_{i+1}, G_{i+1}, T_{i+1}) = (A_i, C_i, G_i, T_i) \begin{pmatrix} 1-\mu/n & \mu/(3*n) & \mu/(3*n) & \mu/(3*n) \\ \mu/(3*n) & 1-\mu/n & \mu/(3*n) & \mu/(3*n) \\ \mu/(3*n) & \mu/(3*n) & 1-\mu/n & \mu/(3*n) \\ \mu/(3*n) & \mu/(3*n) & \mu/(3*n) & 1-\mu/n \end{pmatrix} \quad (10)$$

247 Carrying out the matrix multiplication gives us the four recursion equations which describe this
 248 evolutionary Markov process for the stationary and non-stationary models respectively:

$$249 \quad A_{i+1} = A_i(1-\mu) + C_i*\mu/3 + G_i*\mu/3 + T_i*\mu/3 \quad (11)$$

$$250 \quad C_{i+1} = A_i*\mu/3 + C_i(1-\mu) + G_i*\mu/3 + T_i*\mu/3 \quad (12)$$

$$251 \quad G_{i+1} = A_i*\mu/3 + C_i*\mu/3 + G_i(1-\mu) + T_i*\mu/3 \quad (13)$$

252 $T_{i+1} = A_i*\mu/3 + C_i*\mu/3 + G_i*\mu/3 + T_i(1-\mu)$ (14)

253 And

254 $A_{i+1} = A_i(1-\mu/n) + C_i*\mu/(3*n) + G_i*\mu/(3*n) + T_i*\mu/(3*n)$ (15)

255 $C_{i+1} = A_i*\mu/(3*n) + C_i(1-\mu/n) + G_i*\mu/(3*n) + T_i*\mu/(3*n)$ (16)

256 $G_{i+1} = A_i*\mu/(3*n) + C_i*\mu/(3*n) + G_i(1-\mu/n) + T_i*\mu/(3*n)$ (17)

257 $T_{i+1} = A_i*\mu/(3*n) + C_i*\mu/(3*n) + G_i*\mu/(3*n) + T_i(1-\mu/n)$ (18)

258 The initial condition for either version using equation (6) is:

259 $E_0 = (A_0, C_0, G_0, T_0) = (0,0,0,1)$ (19)

260 It is assumed that for the Jukes-Cantor model, T is the base at the particular site and for the
261 Kishony Mega-Plate experiment that the initial inoculate at time = 0, the bacterium has a T base
262 where an A base is needed to give resistance. The fundamental difference between the
263 stationary and non-stationary models is that as the population size grows, n is increasing in the
264 non-stationary model. The stationary process assumes that the population size is constant (n=1)
265 for all time.

266 FORTRAN computer programs were written to evaluate both stationary and non-stationary
267 versions and compared for two different mutation rates, $\mu = 1E-5$ and $\mu = 1E-9$ and, are
268 presented in the **Results** section. An equivalent calculation was carried out based on two-site
269 models for stationary and non-stationary Markov processes.

270 The Markov Process for Two Sites, the Jukes-Cantor stationary model and the Modified Jukes-
271 Cantor non-stationary model.

272 The analysis for the DNA evolutionary process for two sites begins with the construction of the
273 state transition diagram for the evolution at two sites (Figure 2). This diagram is much more
274 complex in that there are 16 possible states. (Note that only the transition lines to and from state
275 A1A2 to the other states are included in this figure. Transition lines from the other states would
276 appear similarly). In Figure 2, the possible state transitions are drawn for a member of the
277 population which has an A base at site 1 and an A base at site 2 and the possible transitions that
278 can occur on replication. An A1A2 member can replicate and produce another A1A2 member, or
279 an A1C2, or a C1A2, or any of 13 other possible transitions.

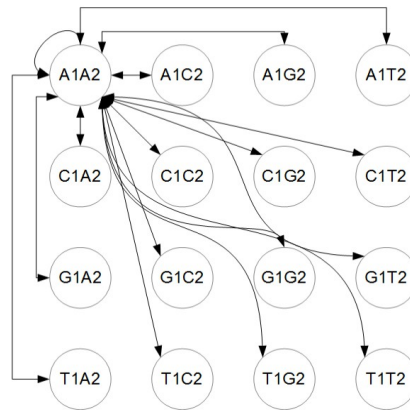


Illustration 2: The two-site Transition Diagram, only A1A2 transition lines shown, similar transition lines for other states apply but not shown.

280 The illustration in Figure 3 gives the diagram for a single state with the understanding that
 281 equivalent states exist for the other possible combinations of bases. The number following the
 282 base letter indicates the site.

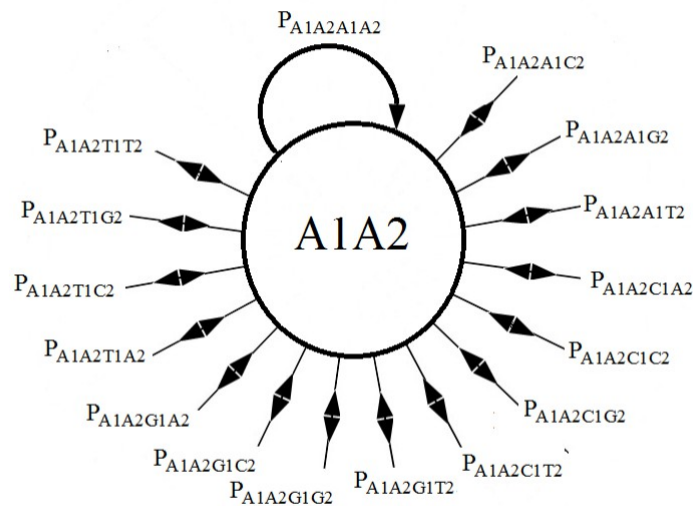


Illustration 3: Possible state transitions for two sites from an A at site 1 and an A at site 2 to all other possible transitional states.

283 In contrast with the single-site model which has 4 possible states and 4 possible transitions from
 284 each state, the two-site (second-order) model has 16 possible states with 16 possible transitions
 285 from each state to the other possible states. The list of possible transitions for the A state for the
 286 single-site model gives 4 probabilities, p_{AA} , p_{AC} , p_{AG} , and p_{AT} . The transition probabilities for the
 287 A1A2 state for the two-site model is, $p_{A1A2A1A2}$, $p_{A1A2A1C2}$, $p_{A1A2A1G2}$, $p_{A1A2A1T2}$, $p_{A1A2C1A2}$, $p_{A1A2C1C2}$, $p_{A1A2C1G2}$,
 288 $p_{A1A2C1T2}$, $p_{A1A2G1A2}$, $p_{A1A2G1C2}$, $p_{A1A2G1G2}$, $p_{A1A2G1T2}$, $p_{A1A2T1A2}$, $p_{A1A2T1C2}$, $p_{A1A2T1G2}$, and $p_{A1A2T1T2}$. Similar
 289 probabilities are obtained for the other 240 possible state transitions in the two-site model. A
 290 $p_{A1A2A1A2}$ transition means that an A base is at site 1 and an A base is at site 2 in the parent, and
 291 that on replication, the descendant will also have an A base at site 1 and an A base at site 2, no
 292 mutation has occurred on replication at either site. A $p_{A1A2A1C2}$ transition means that an A base is
 293 at site 1 and an A base is at site 2 in the parent and that on replication, the descendant will also
 294 have an A base at site 1 but a C base at site 2, no mutation has occurred on replication at site 1
 295 but a C mutation has occurred at site 2. A $p_{A1A2C1G2}$, transition means that an A base is at site 1 and
 296 an A base is at site 2 in the parent and that on replication, the descendant will have a C base at
 297 site 1 and a G base at site 2, a C mutation has occurred on replication at site 1 and a G mutation
 298 has occurred at site 2. And so on for the other possible transitions.

299 For the evolution of two sites, a 16x16 transition matrix is obtained which is partially displayed
 300 in equation (20).

$$301 \quad P = \begin{pmatrix} p_{A1A2A1A2} & p_{A1A2A1C2} & p_{A1A2A1G2} & p_{A1A2A1T2} & p_{A1A2C1A2} & p_{A1A2C1C2} & p_{A1A2C1G2} & p_{A1A2C1T2} & p_{A1A2G1A2} & p_{A1A2G1C2} & p_{A1A2G1G2} & p_{A1A2G1T2} & p_{A1A2T1A2} & p_{A1A2T1C2} & p_{A1A2T1G2} & p_{A1A2T1T2} \\ p_{A1C2A1A2} & p_{A1C2A1C2} & p_{A1C2A1G2} & p_{A1C2A1T2} & p_{A1C2C1A2} & p_{A1C2C1C2} & p_{A1C2C1G2} & p_{A1C2C1T2} & p_{A1C2G1A2} & p_{A1C2G1C2} & p_{A1C2G1G2} & p_{A1C2G1T2} & p_{A1C2T1A2} & p_{A1C2T1C2} & p_{A1C2T1G2} & p_{A1C2T1T2} \\ \dots & \dots & \dots & \dots & \dots & \dots & \dots & \dots & \dots & \dots & \dots & \dots & \dots & \dots & \dots & \dots \\ 302 & & & & & & & & & & & & & & & \\ p_{T1T2A1A2} & p_{T1T2A1C2} & p_{T1T2A1G2} & p_{T1T2A1T2} & p_{T1T2C1A2} & p_{T1T2C1C2} & p_{T1T2C1G2} & p_{T1T2C1T2} & p_{T1T2G1A2} & p_{T1T2G1C2} & p_{T1T2G1G2} & p_{T1T2G1T2} & p_{T1T2T1A2} & p_{T1T2T1C2} & p_{T1T2T1G2} & p_{T1T2T1T2} \end{pmatrix} \quad (20)$$

303 If n is assumed constant and equal to 1, the first row of the two-site transition matrix in terms of
 304 the mutation rate give the Jukes-Cantor stationary version of the two-site model:

305 $p_{A1A2A1A2} = (1-\mu)(1-\mu)$

306 $p_{A1A2A1C2} = (1-\mu)*\mu/3$

307 $p_{A1A2A1G2} = (1-\mu)*\mu/3$

308 $p_{A1A2A1T2} = (1-\mu)*\mu/3$

309 $p_{A1A2C1A2} = (1-\mu)*\mu/3$

310 $p_{A1A2C1C2} = \mu^2/9$

311 $p_{A1A2C1G2} = \mu^2/9$

312 $p_{A1A2C1T2} = \mu^2/9$

313 $p_{A1A2G1A2} = (1-\mu)*\mu/3$

314 $p_{A1A2G1C2} = \mu^2/9$

315 $p_{A1A2G1G2} = \mu^2/9$

316 $p_{A1A2G1T2} = \mu^2/9$

317 $p_{A1A2T1A2} = (1-\mu)*\mu/3$

318 $p_{A1A2T1C2} = \mu^2/9$

319 $p_{A1A2T1G2} = \mu^2/9$

320 $p_{A1A2T1T2} = \mu^2/9$

321 The other rows of the transition matrix from the 240 other possible state transitions will have
 322 similar probabilities. These values are substituted into the two-site transition matrix for the
 323 Jukes-Cantor two-site stationary model. This 16x16 matrix is partially displayed in equation
 324 (21).

325
$$P = \begin{pmatrix} (1-\mu)(1-\mu) & (1-\mu)*\mu/3 & (1-\mu)*\mu/3 & (1-\mu)*\mu/3 & (1-\mu)*\mu/3 & \mu^2/9 & \mu^2/9 & \mu^2/9 & (1-\mu)*\mu/3 & \mu^2/9 & \mu^2/9 & \mu^2/9 & (1-\mu)*\mu/3 & \mu^2/9 & \mu^2/9 & \mu^2/9 \\ (1-\mu)*\mu/3 & (1-\mu)(1-\mu) & (1-\mu)*\mu/3 & (1-\mu)*\mu/3 & \mu^2/9 & (1-\mu)*\mu/3 & \mu^2/9 & \mu^2/9 & \mu^2/9 & (1-\mu)*\mu/3 & \mu^2/9 & \mu^2/9 & \mu^2/9 & (1-\mu)*\mu/3 & \mu^2/9 & \mu^2/9 \\ \dots & \dots & \dots & \dots & \dots & \dots & \dots & \dots & \dots & \dots & \dots & \dots & \dots & \dots & \dots & \dots \\ \mu^2/9 & \mu^2/9 & \mu^2/9 & (1-\mu)*\mu/3 & \mu^2/9 & \mu^2/9 & \mu^2/9 & (1-\mu)*\mu/3 & \mu^2/9 & \mu^2/9 & \mu^2/9 & (1-\mu)*\mu/3 & (1-\mu)*\mu/3 & (1-\mu)*\mu/3 & (1-\mu)*\mu/3 & (1-\mu)(1-\mu) \end{pmatrix}$$

326 (21)

327 The Jukes-Cantor two-site non-stationary model has the following transition probabilities based
 328 on the same reasoning for the single-site model. The probabilities for the A1A2 state are written
 329 as:

330 $p_{A1A2A1A2} = (1-\mu/n)(1-\mu/n)$

331 $p_{A1A2A1C2} = (1-\mu/n)*\mu/(3*n)$

332 $p_{A1A2A1G2} = (1-\mu/n)*\mu/(3*n)$

333 $p_{A1A2A1T2} = (1-\mu/n)*\mu/(3*n)$

334 $p_{A1A2C1A2} = (1-\mu/n)*\mu/(3*n)$

335 $p_{A1A2C1C2} = \mu^2/(3*n)^2$

336 $p_{A1A2C1G2} = \mu^2/(3*n)^2$

337 $p_{A1A2C1T2} = \mu^2/(3*n)^2$

338 $p_{A1A2G1A2} = (1-\mu/n)*\mu/(3*n)$

339 $p_{A1A2G1C2} = \mu^2/(3*n)^2$

340 $p_{A1A2G1G2} = \mu^2/(3*n)^2$

341 $p_{A1A2G1T2} = \mu^2/(3*n)^2$

342 $p_{A1A2T1A2} = (1-\mu/n)*\mu/(3*n)$

343 $p_{A1A2T1C2} = \mu^2/(3*n)^2$

344 $p_{A1A2T1G2} = \mu^2/(3*n)^2$

345 $p_{A1A2T1T2} = \mu^2/(3*n)^2$

346 The other rows of the non-stationary transition matrix from the 240 other possible state
 347 transitions have similar probabilities. These values are substituted into the two-site transition

348 matrix for the Jukes-Cantor two-site non-stationary model. This 16x16 matrix is partially
 349 displayed in equation (22).

$$P = \begin{pmatrix}
 (1-\mu/n)(1-\mu/n) & (1-\mu/n)*\mu/(3*n) & (1-\mu/n)*\mu/(3*n) & (1-\mu/n)*\mu/(3*n) & (1-\mu/n)*\mu/(3*n) & (\mu/(3*n))^2 & (\mu/(3*n))^2 & (\mu/(3*n))^2 & (1-\mu/n)*\mu/(3*n) & (\mu/(3*n))^2 & (\mu/(3*n))^2 & (\mu/(3*n))^2 & (1-\mu/n)*\mu/3 \\
 (1-\mu)*\mu/3 & (1-\mu/n)(1-\mu/n) & (1-\mu/n)*\mu/3 & (1-\mu/n)*\mu/3 & (\mu/(3*n))^2 & (1-\mu/n)*\mu/(3*n) & (\mu/(3*n))^2 & (\mu/(3*n))^2 & (\mu/(3*n))^2 & (1-\mu/n)*\mu/(3*n) & (\mu/(3*n))^2 & (\mu/(3*n))^2 & \mu^2/9 \\
 \dots & \dots & \dots & \dots & \dots & \dots & \dots & \dots & \dots & \dots & \dots & \dots & \dots \\
 (\mu/(3*n))^2 & (\mu/(3*n))^2 & (\mu/(3*n))^2 & (1-\mu/n)*\mu/(3*n) & (\mu/(3*n))^2 & (\mu/(3*n))^2 & (\mu/(3*n))^2 & (1-\mu/n)*\mu/3 & (\mu/(3*n))^2 & (\mu/(3*n))^2 & (\mu/(3*n))^2 & (1-\mu/n)*\mu/(3*n) & (1-\mu/n)*\mu/(3*n)
 \end{pmatrix}$$

350
 351 (22)

352 In a similar manner as with the single-site model, the state transition equation is:

$$353 E_{i+1} = E_i P \tag{23}$$

354 Equations (21) and (22) are used for the stationary and non-stationary models (and the 15 other
 355 equivalent transition equations) and the two-site transition matrix to compute the Markov chain
 356 recursion equations.

357 (Note that when X1Y2 where X and Y can be A, C, G, or T are italicized indicates the frequencies
 358 of those variants with X at site 1 and Y at site 2.) The recursion equation for the A1A2 state
 359 Jukes-Cantor stationary model is:

$$360 A1A2_{i+1} = A1A2_i*(1-\mu)^2 + (A1C2_i + A1G2_i + A1T2_i + C1A2_i + G1A2_i + T1A2_i)*(1-\mu)*\mu/3 + (C1C2_i +
 361 C1G2_i + C1T2_i + G1C2_i + G1G2_i + G1T2_i + T1C2_i + T1G2_i + T1T2_i)*\mu^2/9 \tag{24}$$

362 Equivalent equations are obtained for the other 15 states. The equivalent recursion equation for
 363 the A1A2 state Jukes-Cantor non-stationary model is:

$$364 A1A2_{i+1} = A1A2_i*(1-\mu/n)^2 + (A1C2_i + A1G2_i + A1T2_i + C1A2_i + G1A2_i + T1A2_i)*(1-\mu/n)*\mu/(3*n) +
 365 (C1C2_i + C1G2_i + C1T2_i + G1C2_i + G1G2_i + G1T2_i + T1C2_i + T1G2_i + T1T2_i)*(\mu/(3*n))^2 \tag{25}$$

366 Similar equations for the other 15 possible states give the full definition of the Markov
 367 transformation for the non-stationary model.

368 The initial state for either two-site system is written:

$$369 E_0 = (A1A2_0, A1C2_0, A1G2_0, A1T2_0, C1A2_0, C1C2_0, C1G2_0, C1T2_0, G1A2_0, G1C2_0, G1G2_0, G1T2_0, T1A2_0,
 370 T1C2_0, T1G2_0, T1T2_0) \tag{26}$$

371 The $A1A2_0, \dots, T1T2_0$ terms are the frequencies of the particular variant in the initial state. The
 372 state of the system at time t_{i+1} is given by equation (23).

373 It is assumed that in the initial state, the wild type variant inoculated on the plate for a two-drug
 374 experiment has bases T at site 1 and at site 2 such that $T1T2_0 = 1$ (that is the frequency of that
 375 variant is 1) and the other 15 possible states $A1A2_0, \dots, T1G2_0 = 0$ gives an initial condition of:

$$376 E_0 = (0, 0, 0, 0, 0, 0, 0, 0, 0, 0, 0, 0, 0, 0, 0, 1) \tag{27}$$

377 The stationary and non-stationary two-site models were evaluated similarly as the single-site
 378 models and compared for two different mutation rates, $\mu = 1E-5$ and $\mu = 1E-9$, and presented in
 379 the **Results** section.

380 Results

381 The Numerical Calculation of the Jukes-Cantor single-site Stationary and Non-stationary

382

Models

383 FORTRAN computer programs were written to compute the values for equations (11-14)
384 stationary model and equations (15-18) non-stationary model for two mutation rates, 1E-5 and
385 1E-9. The FORTRAN source code is supplied in the supplemental documentation as well as the
386 data derived from these programs. The results are shown in the graphs below for the Jukes-
387 Cantor stationary and non-stationary models for two mutation rates. The first two figures are for
388 the single site stationary systems (mutation rates 1E-5 and 1E-9 respectively).

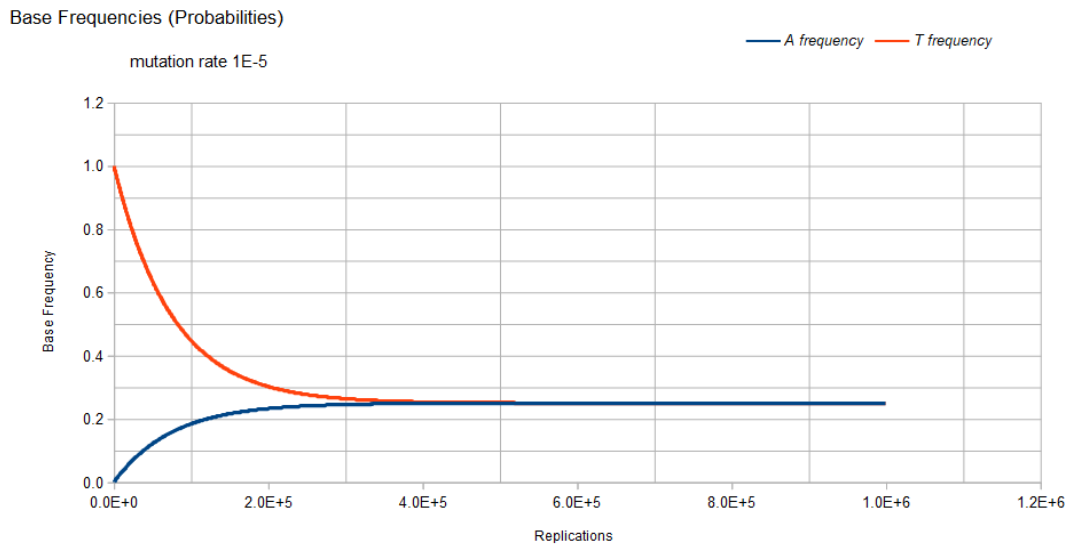


Illustration 4: Base frequencies for A and T variants, Jukes-Cantor stationary model, single-site, as a function of number of replications and mutation rate 1E-5

389 The base frequencies for the C and G variants are not included in Figure 4 because these base
390 frequencies are identical to the A frequency curve. This is because of the symmetry of the Jukes-
391 Cantor model. The mutation rate for base transitions is the same for base transversions. Each
392 Markov transition in the Jukes-Cantor stationary model is both a replication and a generation.
393 Each element in the transition matrix is the mutation rate for a particular mutational change in a
394 single replication for a single member of a lineage. Therefore, each replication is also a
395 generation.

396 The way to correlate the curves in Figure 4 to the genetic transformation is to consider some
397 founder bacterium of a lineage in the population with a T base at a particular site in the genome.
398 That bacterium replicates, and its descendant will have a slightly reduced probability of a T base
399 at that site and a slightly increased probability of having an A, C, or G base (mutation) at that site.
400 When that descendant replicates, its descendant will have another slight decrease in the
401 probability of a T base occurring at that site and another slight increase in the probability of

402 having an A, C, or G mutation at that site. Each replication of the following descendants will
403 decrease the probability of T occurring at that site and increase the probability of an A, C, or G
404 mutation at that site until the evolutionary process reaches equilibrium where the probability of
405 any of the four possible bases occurring at that site will be 0.25. For the mutation rate of $1E-5$,
406 this occurs at about $4E5$ replications (generations). After $4E5$ replications, the probability of
407 finding any of the four bases at that site remains constant at the value of 0.25. This evolutionary
408 model has reached equilibrium.

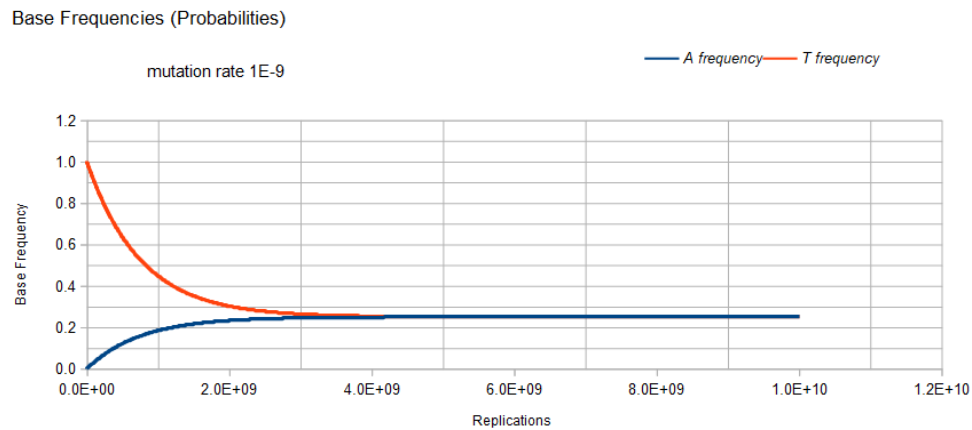


Illustration 5: Base frequencies for A and T variants, Jukes-Cantor stationary model, single-site, as a function of number of replications and mutation rate $1E-9$

410 Figure 5 demonstrates the result of the Jukes-Cantor stationary model similar to Figure 4 except
411 with a lower mutation rate. As with Figure 4, Figure 5 does not include the C and G frequency
412 (probability) curves because these base frequencies are identical to the A frequency curve. The
413 same Markov DNA evolutionary process described in Figure 4 is occurring with the case whose
414 result is illustrated in Figure 5. The only difference is that the lower mutation rate ($1E-9$ vs. $1E-5$)
415 results in a slower approach to equilibrium ($4E9$ vs. $4E5$ replications), but either case
416 converges on the same equilibrium values for the base frequencies, 0.25.

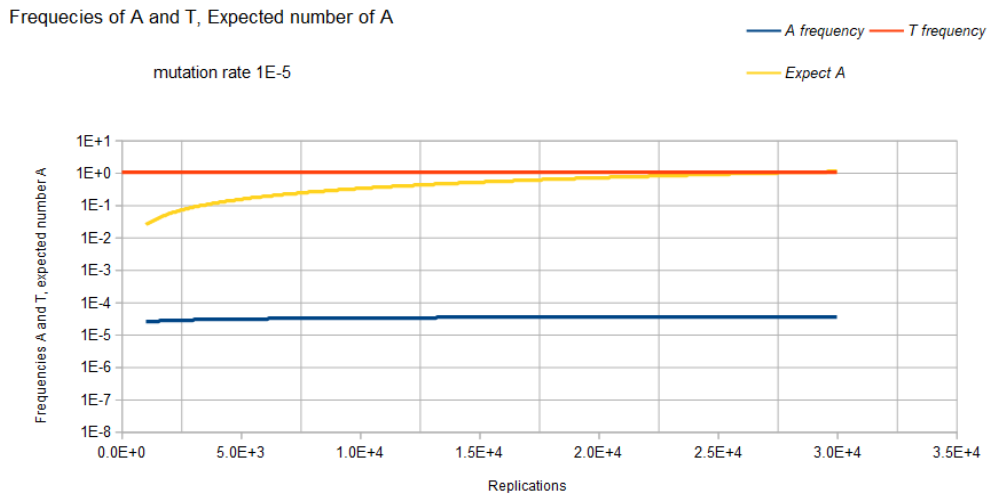


Illustration 6: Base frequencies for A and T variants and expected number of A, Jukes-Cantor non-stationary model, single-site, as a function of number of replications and mutation rate 1E-5.

418 Figure 6 gives the result of the Jukes-Cantor non-stationary model of DNA evolution. It is this
419 model that is proposed to be the correct simulation of the Kishony Mega-Plate experiment. As
420 with the Jukes-Cantor stationary model, as described in Figures 4 and 5, the frequencies
421 (probabilities) for the C and G variants are not plotted because these base frequencies give
422 identical curves to the A frequency curve. In this case, each replication is not a generation. To
423 understand this graph (and mathematics) in the context of the Kishony Mega-Plate experiment,
424 consider what happens from the start of the initial condition of the experiment.

425 Initially, a non-drug resistant bacterium is inoculated into the drug-free region of the petri dish.
426 In this case, it is assumed that the base at the site of interest is T. Initially, the frequency of that
427 variant is 1, and the frequency of any variant with an A, C, or G base at that site is 0. That
428 bacterium double for the first generation. The Markov transition matrix for that single
429 replication gives a small probability that an A, C, or G mutation occurs, and the probability that a
430 T occurs is slightly less than 1. These two bacteria double for the second generation. It requires 2
431 Markov transitional steps to compute the frequencies of the different variants for this
432 generation. Each of these Markov transitional steps slightly reduces the frequency of the T
433 variants and slightly increases the frequencies of the A, C, and G variants. The next generation
434 consists of a doubling of these four bacteria to 8 bacteria that requires 4 Markov transitional
435 steps to compute the frequencies of each of the different variants for this generation. This DNA
436 evolutionary process continues until the frequency of A, and the total population size is
437 sufficient to give an expected occurrence of an A variant ($n_A = n * A$). For a mutation rate of 1E-5,
438 this occurs at about a population size of 3E4 (about 15 doublings or generations).

439 Another consideration is that this Markov process is occurring at every site in the genome of the
440 bacteria used by the Kishony team. Two different antimicrobial agents were used (not
441 simultaneously) in the experiment, Ciprofloxacin, and Trimethoprim. The occurrence of
442 resistance mutations to either drug occurs in a single colony which is demonstrated by the use of

443 either drug in the experiment. The experiment does not work when both drugs are used
444 simultaneously [18]. In order for the experiment to work with 2 drugs requires that a single
445 variant have resistance mutations for both drugs. The mathematical requirement for this to
446 occur is demonstrated by the 2 sites non-stationary Markov process.

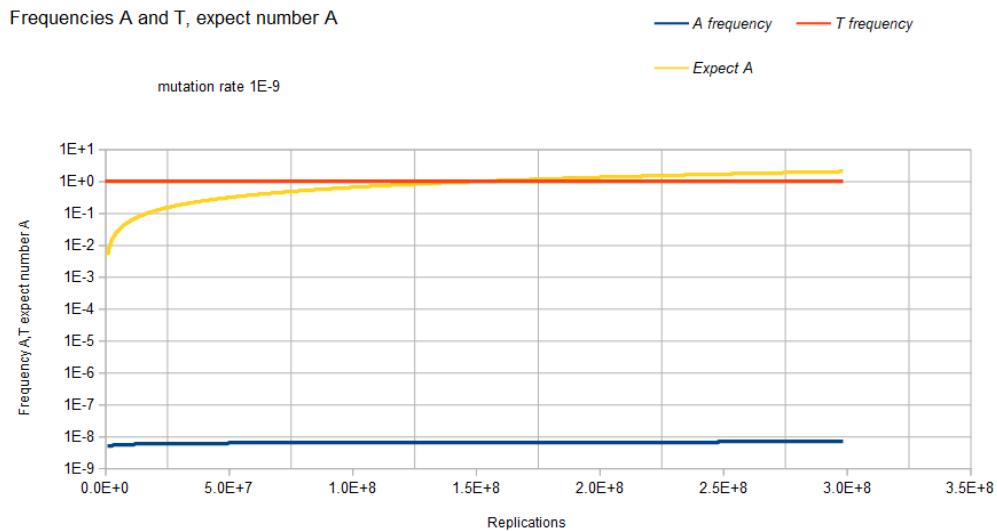


Illustration 7: Base frequencies for A and T and expected number of variant A, Jukes-Cantor non-stationary model, single-site, mutation rate 1E-9.

448 Figure 7 demonstrates the results of the Jukes-Cantor non-stationary model similar to Figure 6
449 except with a lower mutation rate. As with Figure 6, Figure 7 does not include the C and G
450 frequency (probability) curves because these base frequencies are identical to the A frequency
451 curve. The same Markov DNA evolutionary process that is described in Figure 6 is occurring
452 with this case whose result is illustrated in Figure 7. The only difference is that the lower
453 mutation rate (1E-9 vs. 1E-5) results in a slower approach to an expected occurrence of variant
454 A equal to 1. (1.5E8 (about 28 doublings or generations) vs. 3E4 replications (about 15
455 doublings or generations)).

456 The following four figures show the results for the two site Jukes-Cantor model, the first two of
457 these four are for the stationary two sites model, mutation rates 1E-5 and 1E-9 respectively, and
458 the last two figures for the two sites non-stationary model, mutation rates 1E-5 and 1E-9
459 respectively.

460 FORTRAN computer programs were written to compute the values for equation (25) (plus the
461 15 other equivalent equations) stationary model and equation (26) (plus the 15 other equivalent
462 equations) non-stationary model for two mutation rates, 1E-5, and 1E-9. The results are shown
463 in the following two graphs below for the two sites Jukes-Cantor model (mutation rate 1E-5 and
464 1E-9 respectively). Source code and computed data are included in supplementary
465 documentation.

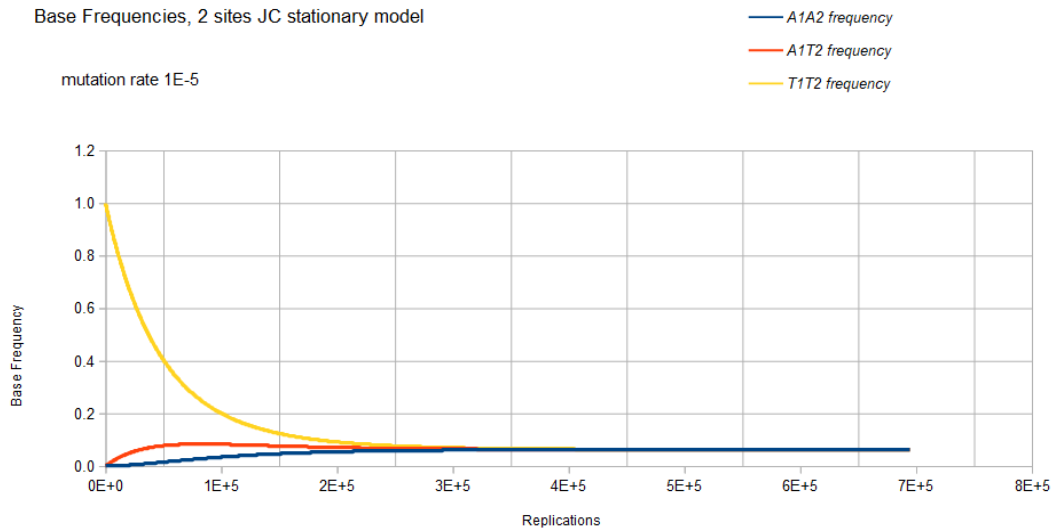


Illustration 8: Base frequencies for A1A2, A1T2, and T1T2 variants, Jukes-Cantor stationary model, two sites, as a function of number of replications and mutation rate 1E-5

466 The base frequencies for the X1Y2 variants where neither X nor Y is a T base are not included in
467 Figure 8 because these base frequencies are identical to the A1A2 frequency curve. The base
468 frequencies for the X1T2 and T1Y2 variants where neither X nor Y is a T base are not included in
469 Figure 8 because these base frequencies are identical to the A1T2 frequency curve. This is again
470 because of the symmetry of the Jukes-Cantor model. The mutation rate for base transitions is the
471 same for base transversions. Each Markov transition in the Jukes-Cantor stationary model is
472 both a replication and a generation. Each element in the transition matrix is the product of the
473 individual mutation rates (that is the joint probability) of the particular mutational change at
474 each site in a single replication for a single member of a lineage. Therefore, each replication is
475 also a generation.

476 The way to correlate the curves in Figure 8 to the genetic transformation is to consider a
477 bacterium in a population with a T1 base at one particular site and a T2 base at another
478 particular site in the genome. That bacterium replicates, and its descendant will have a slightly
479 reduced probability of either a T1 base at the one particular site or a T2 base at the other
480 particular site and a slightly increased probability of having an A1, A2, C1, C2, G1, or G2 base
481 (mutation) at their particular sites. When that descendant replicates, its descendant will have
482 another slight decrease in the probability of a T1 or T2 base occurring at their particular sites
483 and another slight increase in the probability of having an A1, A2, C1, C2, G1, or G2 mutation at
484 their particular sites. Each replication of each of the following descendants will decrease the
485 probability of T1 or T2 occurring at the particular sites and increase the probability of an A1, A2,
486 C1, C2, G1, or G2 mutation at their particular sites until the evolutionary process reaches
487 equilibrium where the probability of any of the eight possible bases (four possible bases at each
488 site) occurring at that site will be 0.0625. For the mutation rate of 1E-5, this occurs at about 4E5
489 replications (generations). After 4E5 replications, the probability of finding any of the eight
490 possible bases at the two particular sites remains constant at the value of 0.0625. This
491 evolutionary model has reached equilibrium.

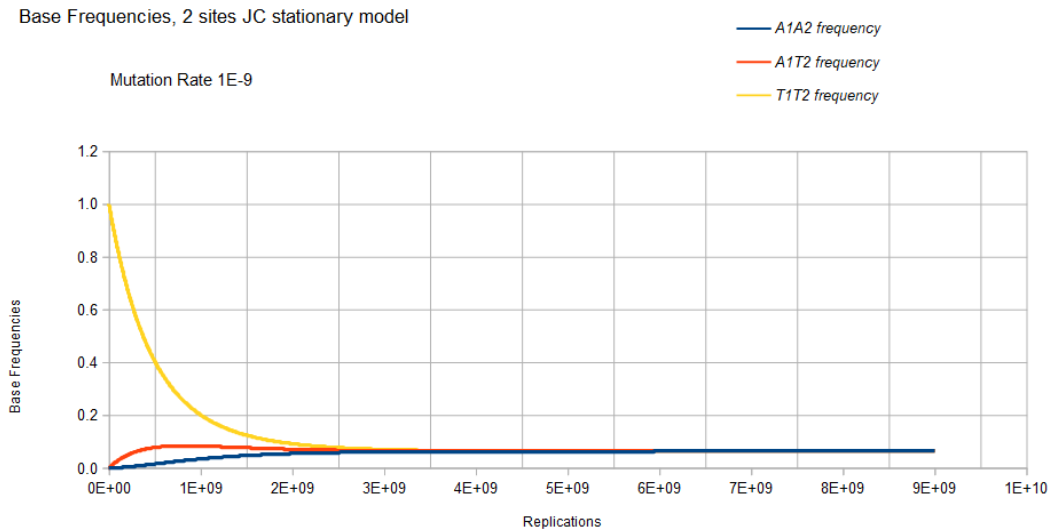


Illustration 9: Base frequencies for A1A2, A1T2, and T1T2 variants, Jukes-Cantor stationary model, two sites, as a function of number of replications and mutation rate 1E-9

493 Figure 9 demonstrates the result of the Jukes-Cantor two-site stationary model similar to Figure
494 8 except with a lower mutation rate. As with Figure 8, Figure 9 does not include most of the base
495 frequencies for the same reason, as described in Figure 8. The only difference is that the lower
496 mutation rate (1E-9 vs. 1E-5) results in a slower approach to equilibrium (4E9 vs. 4E5
497 replications (generations)), but either two sites stationary case converges on the same
498 equilibrium values for the base frequencies, 0.0625.

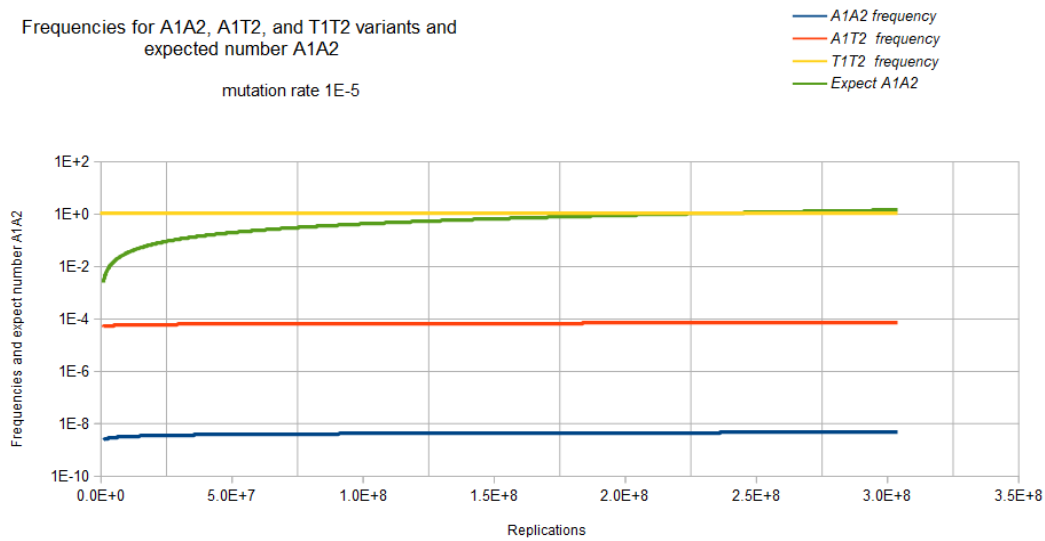


Illustration 10: Base frequencies for A1A2, A1T2, and T1T2 variants, and expected number of A1A2 variants, Jukes-Cantor non-stationary model, two sites, as a function of number of replications and mutation rate 1E-5.

499 Figure 10 gives the result of the Jukes-Cantor two-site non-stationary model of DNA evolution.
 500 The base frequencies for the X1Y2 variants where neither X nor Y is a T base are not included in
 501 Figure 10 because these base frequencies are identical to the A1A2 frequency curve. The base
 502 frequencies for the X1T2 and T1Y2 variants where neither X nor Y is a T base are not included in
 503 Figure 10 because these base frequencies are identical to the A1T2 frequency curve. This is
 504 again because of the symmetry of the Jukes-Cantor model. The mutation rate for base transitions
 505 is the same for base transversions. Each Markov transition in the Jukes-Cantor 2 site non-
 506 stationary model is only a replication, not a generation. Each element in the transition matrix is
 507 the product of the individual mutation rates (that is the joint probability) of the particular
 508 mutational change at each site in a single replication where the change in frequencies of the
 509 different variants now depends on population size.

510 Consider the math presented here in the context if the Kishony team tries to perform the
 511 experiment with two drugs (or if the step increase in drug concentration is so large that two
 512 mutations are required for adaptation to the next higher drug concentration region). Initially, a
 513 single non-drug resistant bacterium is inoculated into the drug-free region of the petri dish. In
 514 this case, it is assumed that the base at one site of interest is T1 and for the second site of
 515 interest the base is T2 so that the frequency of that T1T2 variant is 1 and the frequency of any
 516 variant with combinations A1, A2, C1, C2, G1 or G2 base at sites 1 and 2 are 0. That bacterium
 517 double for the first generation. The Markov transition matrix for that single replication gives a
 518 small probability that an A, C, or G mutation occurs at either site and the probability that a T
 519 occurs at either site is slightly less than 1. These two bacteria double for the second generation.
 520 This requires 2 Markov transitional steps to compute the frequencies of the different possible
 521 variants. Each of these Markov transitional steps slightly reduce the frequency of the T1T2
 522 variant and very slightly increase the frequencies of the A1A2, A1C2, A1G2, C1A2, C1C2, C1G3,
 523 G1A2, G1C2, and G1G2 variants and slightly increase the frequencies of the A1T2, C1T2, G1T2,

524 T1A2, T1C2, and T1G2 variants. The next generation consists of a doubling of these four bacteria
525 to eight bacteria which requires 4 Markov transitional steps to compute the frequencies of each
526 of the different variants. This DNA evolutionary process continues until the frequency of A1A2
527 (the assumed double drug resistant variant) and the total population size is sufficient to give an
528 expected occurrence of an A1A2 variant ($nA1A2=n \cdot A1A2$). For a mutation rate of $1E-5$ this
529 occurs at about a population size of $2.3E8$ (about 28 doublings or generations).

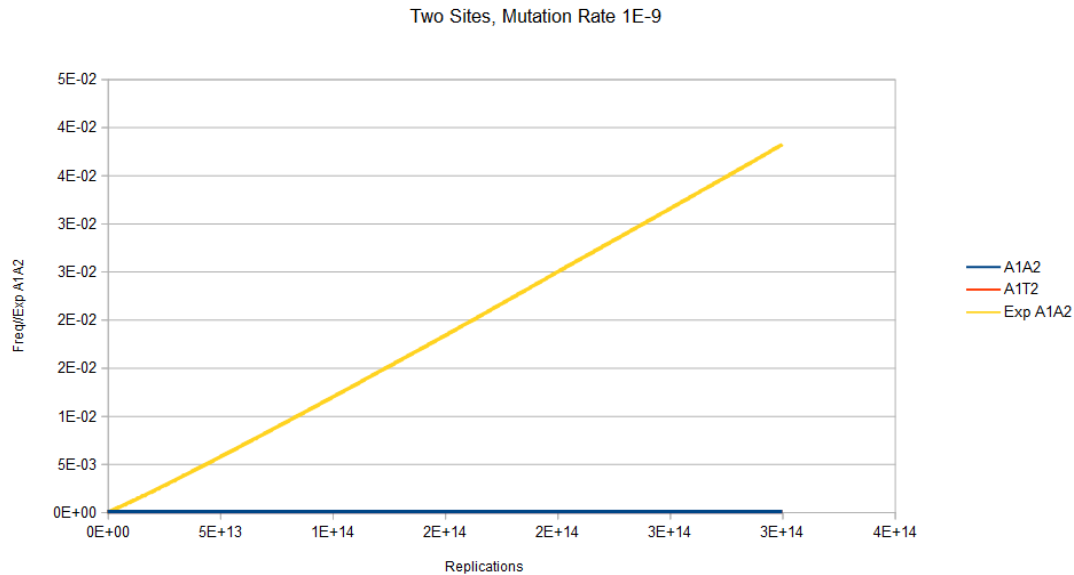


Illustration 11: Base frequencies for A1A2 and A1T2 variants, and expected number of A1A2 variant, Jukes-Cantor non-stationary model, two sites, as a function of number of replications and mutation rate $1E-9$

530 Figure 11 gives the result of the Jukes-Cantor 2 site non-stationary model similar to Figure 10
531 except with a lower mutation rate. As with Figure 10, Figure 11 does not include A1C2, A1G2,
532 C1A2, C1C2, C1G2, G1A2, G1C2, and G1G2 frequency curves because these base frequencies are
533 identical with the A1A2 frequency curve. The base frequencies for the C1T2, G1T2, T1A2, T1C2,
534 and T1G2 variants are not included in Figure 11 because these base frequencies are identical to
535 the A1T2 frequency curve. The frequency of the T1T2 variant remains very close to 1, only very
536 slowly decreasing as the number of replications increases so it is not displayed. The A1A2
537 frequency curve appears superimposed on the A1T2 curve because of the very small values (of
538 the order of $1E-16$ and $1E-8$ respectively). The expected occurrence of an A1A2 variant is very
539 slowly increasing and the computation was halted at $3E14$ replications (about 48 doublings
540 (generations)). A linear interpolation of the data from Figure 11 gives the expected occurrence
541 of an A1A2 variant will occur at about $8E15$ replications (about 53 doublings of the original
542 founder bacterium). For the Kishony Mega-Plate experiment to work with two drugs (or a larger
543 step increase in drug-concentration), a much, much larger petri dish will be needed than the
544 "Mega-Plate".

545 Discussion/Conclusion

546 The mathematical behavior of the Markov process of DNA evolution is significantly different
547 when assuming a stationary versus a non-stationary model. It is shown that the Jukes-Cantor
548 model assumes a constant population size of 1 because of the elements used in the transition

549 matrix. The Jukes-Cantor stationary model is physically modeling a single-site in the DNA in a
550 lineage of a single member of a population. Because of this, each transition from one state to the
551 next represents a generation. The initial state at that site, the probability (frequency) of that
552 base is 1, and the probability of any of the other bases is 0. When that member replicates, the
553 probability of the original base occurring is slightly less than 1 and the probability of any of the
554 other substitutions now is slightly greater than 0. When that descendant replicates, the
555 probability of the original base is again slightly decreased and the probabilities of any of the
556 possible substitutions are increased. When the equilibrium state is achieved, the probabilities of
557 finding any of the possible bases will be 0.25 for all possible bases. And the number of
558 replications to reach that state is approximately $1/(1/4 * \mu)$. Once the equilibrium state is reached,
559 with any further replications, the probability of finding any base at that site will be 0.25 no
560 matter how many further replications occur.

561 The Jukes-Cantor model for a single-site converges to a stationary value of 0.25 regardless of the
562 mutation rate, and the two-site model converges to 0.0625 (again regardless of the mutation
563 rate). As with, the single-site Jukes-Cantor model, the equivalent two-site model also applies to
564 the lineage of a single member where each transition represents a replication of that particular
565 member, but that replication also represents a generation. When a constant non-unity
566 population is considered with the model, each matrix multiplication still represents a single
567 replication of that member, but now a generation is n matrix multiplications (replications). The
568 non-stationary Jukes-Cantor model takes into account the number of replications (population
569 size) occurring in a lineage. This has a strong effect on the relative frequencies of the different
570 variants in the population. This model does not reach equilibrium. The Kishony Mega-Plate
571 experiment starts its evolutionary process with a single “wild-type” variant. As these wild-type
572 replicates and the population size increases, the relative frequencies are changing, but very
573 slowly, and most of the members of the population will have the original base at the site of
574 interest. The probability of the correct mutation occurring is improving as the colony size grows,
575 but its relative frequency will be very low because of the large population size, and this is
576 demonstrated by the non-stationary Jukes-Cantor model as well as the Kishony Mega-Plate
577 Experiment.

578 The single-site Jukes-Cantor stationary model with a mutation rate of $1E-5$ reaches equilibrium
579 and relative frequencies of all variants of 0.25 at about $4E5$ replications, as shown in Figure 4.
580 For the same mutation rate and the number of replications, the single-site Jukes-Cantor non-
581 stationary model shows the relative frequency of the wild-type to be very close to 1, and the
582 relative frequency of the mutated variant to be $6E-5$, but the expected number of the drug-
583 resistant mutated variant will be about 1. Likewise, for a mutation rate of $1E-9$, the single-site
584 Jukes-Cantor stationary model reaches an equilibrium of 0.25 at about $3E9$ replications. This is
585 the same number of replications that on average would give every possible base substitution at
586 every site in a genome. And this is the approximate number of replications for the Kishony
587 populations to get the next beneficial mutation for the next higher drug-concentration region.

588 The reason why such significant differences occur between the stationary and non-stationary
589 models can be seen when equations (4) and (16) are considered, $E_i = (A_i, C_i, G_i, T_i)$ for the single-
590 site model that is identical for both stationary and non-stationary models. E_i is the state of the
591 system at time (generation), i and A_i, C_i, G_i, T_i are the frequencies of the bases in that population
592 at time i . If the total population size is n , and the number of members of the population of each of
593 the variants is $n_{A_i}, n_{C_i}, n_{G_i}, n_{T_i}$ respectively, then frequencies A_i, C_i, G_i, T_i at time i will be $n_{A_i}/n, n_{C_i}/n,$
594 $n_{G_i}/n, n_{T_i}/n$, respectively. In the stationary formulation of the Jukes-Cantor model, n is implicitly

595 assumed to be constant, and equal to 1. In the Kishony Mega-Plate experiment, n is not constant
596 and varies with time. When n is considered to be a function of time as demonstrated above, the
597 non-stationary Jukes-Cantor model will give accurate predictions of this experiment. This
598 principle becomes even more apparent for Markov Chain models of DNA evolution when two
599 sites are being considered simultaneously.

600 The two-site stationary model with a mutation rate of $1E-9$ also reaches equilibrium at about
601 $3E9$ replications and a frequency value of 0.0625. This value under-predicts the number of
602 replications in the Kishony experiment to accumulate the first two beneficial mutations
603 sequentially by a factor of 2. Also, the frequency of the different variants will be nowhere close
604 to 0.0625. In the actual experiment, the frequency of the wild-type is still very close to 1, and the
605 mutated members of the population represent only a small portion of the total population.

606 The non-stationary model with mutation rate $1E-5$ at $2.5E4$ replications shows the wild-type
607 variant still at very close to a relative frequency of 1, the mutant variant at the relative frequency
608 of about $5E-5$, and the expected number of 1 drug-resistant mutant variant in that population.
609 When the mutation rate is lowered to $1E-9$, at $2E8$ replications still shows a relative frequency of
610 the wild-type to be almost 1, and the relative frequency of the mutated variant is still less than
611 $1E-8$, but one would expect there would be one mutated drug-resistant variant in that
612 population. This is demonstrated by the Kishony Mega-Plate experiment. The vast majority of
613 the members in a given colony are not mutated variants that can grow in the next higher drug
614 region, these members are clones of the founder of that colony (at least at that particular site in
615 the genome).

616 If the mutations in any evolutionary Markov process are accumulated sequentially as in the
617 Kishony Mega-Plate experiment, the number of replications required to make the transition is
618 exponentially smaller than when the mutations must be accumulated simultaneously. The
619 mathematical explanation for this is the multiplication rule of probabilities. This is the reason
620 that the Kishony Mega-Plate experiment can only operate with small increases in drug-
621 concentration on the plate used. Any higher concentration of the drug or the use of two or more
622 drugs will require a much, much larger plate to accommodate the much larger colony size
623 necessary for such an evolutionary process.

624 There are two significant points to consider when a single drug is used versus two drugs (or a
625 higher drug-concentration in the adjacent region) in the physical behavior and mathematical
626 modeling of the Kishony Mega-Plate experiment. When an evolutionary process such as the one
627 drug experiment is carried out, the mutations can accumulate sequentially, one at a time. What
628 that means biologically is that some member of the population gets the beneficial mutation that
629 gives improved fitness in a particular colony (lineage). That member is then able to form a new
630 colony in the next higher drug-concentration region and start a new Markov process. It doesn't
631 matter what happens to its progenitor colony. It can continue to grow or go extinct. In the case
632 where two drugs are used or when the drug-concentration in the adjacent band is too large
633 (requiring more than one mutation to grow in that region), a second or higher-order Markov
634 transition matrix is required. What this means numerically and biologically is that the variant
635 with one of the beneficial mutations (after several hundred million replications in that colony)
636 must continue to grow in that colony. That variant with the first beneficial mutation will have to
637 do about 30 doublings (when the mutation rate is $1E-9$) to get the second beneficial mutation
638 necessary to grow in the next higher drug-concentration region. But the other variants will also
639 be doubling at the same time instead of starting with just one member in that lineage it will be

640 one of the other hundreds of millions of other members in that colony. This means the carrying
641 capacity of that environment must be vastly larger to accommodate this much, much larger
642 colony.

643 The importance of understanding DNA evolution cannot be overstated. The impact on the health
644 care system of infectious diseases and the evolution of drug resistance is one of the greatest
645 burdens on the medical system. According to the Healthcare Cost and Utilization Project (HCUP)
646 [19] on the most common medical reasons in 2003 for all hospitalizations that began in the
647 emergency department, pneumonia was the number 1, urinary infections 12, skin infections 15,
648 and sepsis 16. These statistics have not improved with time. According to recent HCUP data
649 (2018) [20], excluding maternal and neonatal stays, the main reasons for hospital admission are,
650 septicemia number 1 and pneumonia number 4. That is only half the story. HCUP 2008 data [21]
651 for the most expensive hospitalization shows the septicemia is the number 1 most expensive
652 cause for hospitalization.

653 How much of this problem is due to the way antibiotics are used in the outpatient environment
654 is unclear. Conflicting signals are given to primary care physicians on the use of antibiotics.
655 Primary care physicians are being warned in the overuse of antibiotics because of the selection
656 of drug resistant variants and killing non-pathogenic bacteria. [22-24] On the other hand, the
657 data from the previous paragraph would seem to indicate that delay or under-use of antibiotics
658 may be occurring. Primary care physicians usually don't have access to stat laboratories to give
659 objective evidence for a disease they are trying to treat in an ill patient. Primary care physicians
660 must depend on the medical history and clinical examination with minimal data, usually just the
661 patient's vital signs and perhaps a rapid in office test such as a rapid group A streptococcal or
662 influenza test. Physicians working in the outpatient environment don't have the benefit of close
663 patient observation such as what occurs with the hospitalized patient. Outpatient physicians
664 must depend upon the patient or family members to report on condition changes and they may
665 not be capable to recognize a worsening condition. In the case of early sepsis, even a 24 hour
666 delay in the initiation of antibiotics can lead to life threatening infections.

667 The discussion does not end here. Drug-resistant infections are a bigger problem in the
668 hospitalized patient than in the out-patient environment. It is well known that community
669 acquired MRSA infections are still sensitive to more antibiotics than hospital acquired MRSA
670 infections. [25] This is most likely due to the fact that hospitalized patients tend to be sicker with
671 weaker immune systems than the generally more healthy out-patients. [26]

672 Based on the analysis of the evolution of drug-resistance in the Kishony Mega-Plate experiment,
673 it is clear that the evolution of drug-resistance to a single drug selection pressure is much easier
674 for a bacterial population to accomplish than evolution to two or more drugs simultaneously.
675 This would seem to point to a better solution of using combination antibiotics rather than not
676 using antibiotics to prevent the selection of resistant variants.

677 DNA evolution can be modeled as a Markov process, but the assumption that this Markov
678 process is stationary leads to inaccurate predictions when doing phylogenetic DNA analysis, or
679 using these models to predict the behavior of evolutionary experiments. The underlying
680 problem with the Jukes-Cantor and derivative models is that in the formulation of these models,
681 it is assumed that the evolutionary process is stationary, and these models don't take into
682 account population size. Implicit in the derivation of the Jukes-Cantor and derivative models is
683 that the substitution matrix does not change. The probabilities in the transition matrix are a
684 function of population size. DNA evolution is not a stationary Markov process, and applying this

685 stationary model selectively to only homologous portions of the genome ignores all the genetic
686 differences that would defeat the accuracy of the predictions this model is capable of doing. By
687 including the population size in the transition matrix, this model will correctly simulate and
688 predict the evolutionary behavior of the Kishony Mega-Plate experiment.

689

690 The evolution of drug-resistance of microbes to drug therapies or cancers to targeted therapies
691 requires an accurate understanding of the evolutionary process. The non-stationary Markov
692 chain model of DNA evolution gives an important tool for understanding evolution. And that tool
693 gives the ability to estimate the number of selection pressures (antibiotics or targeted cancer
694 therapies) necessary to address and suppress the evolutionary process and have a greater
695 probability of having treatment success.

696 **Statements**

697 **Statement of Ethics**

698 No human or animal studies were used in this research. No study approval statement or consent
699 to participate statement required.

700 **Conflict of Interest Statement**

701 “The author have no conflicts of interest to declare.”

702 **Funding Sources**

703 Author self-funded this research.

704 **Author Contributions**

705 Alan Kleinman, MD, PhD is the sole author of this paper.

706 **Data Availability Statement**

707 All data and FORTRAN computer programs used to generate data are available on request in the
708 supplemental documentation.

References

- 709 1. Baym M, Lieberman TD, Kelsic ED, et al. Spatiotemporal microbial evolution on antibiotic
710 landscapes. *Science*. 2016;353(6304):1147-1151. doi:10.1126/science.aag0822
711 <https://www.ncbi.nlm.nih.gov/pmc/articles/PMC5534434/>
- 712 2. Baym M, Gross R, How To Make A MEGA-plate,
713 https://openwetware.org/wiki/How_To_Make_A_MEGA_plate
- 714 3. Kishony R, EXTRA MINUTES - SUPERBUGS (Harvard Experiment explained),
715 https://www.youtube.com/watch?v=Irn6w_Gsas&t=1s
- 716 4. Jukes, T.H. and Cantor, C.R. (1969) Evolution of Protein Molecules. In: Munro, H.N., Ed.,
717 Mammalian Protein Metabolism, Academic Press, New York, 21-132.
718 <http://dx.doi.org/10.1016/B978-1-4832-3211-9.50009-7>
- 719 5. Kimura M., "A simple method for estimating evolutionary rates of base substitutions
720 through comparative studies of nucleotide sequences". *Journal of Molecular Evolution*.
721 16 (2): 111–20. doi:10.1007/BF01731581.
- 722 6. Kimura M., "Estimation of evolutionary distances between homologous nucleotide
723 sequences". *Proceedings of the National Academy of Sciences of the United States of*
724 *America*. 78 (1): 454–8. doi:10.1073/pnas.78.1.454.
- 725 7. Felsenstein J., "Evolutionary trees from DNA sequences: a maximum likelihood
726 approach". *Journal of Molecular Evolution*. 17 (6): 368–76. doi:10.1007/BF01734359.
- 727 8. Hasegawa M, Kishino H, Yano T., "Dating of the human-ape splitting by a molecular clock
728 of mitochondrial DNA". *Journal of Molecular Evolution*. 22 (2): 160–74.
729 doi:10.1007/BF02101694.
- 730 9. Tamura K., "Estimation of the number of nucleotide substitutions when there are strong
731 transition-transversion and G+C-content biases". *Molecular Biology and Evolution*. 9 (4):
732 678–87. doi:10.1093/oxfordjournals.molbev.a040752.
- 733 10. Tamura K, Nei M (May 1993). "Estimation of the number of nucleotide substitutions in
734 the control region of mitochondrial DNA in humans and chimpanzees". *Molecular*
735 *Biology and Evolution*. 10 (3): 512–26. doi:10.1093/oxfordjournals.molbev.a040023.
- 736 11. Casanellas M, Fernández-Sánchez J, Garrote-López, M., "Distance to the stochastic part
737 of phylogenetic varieties", *Journal of Symbolic Computation*, Available online 22
738 September 2020, © 2020 Elsevier Ltd, doi:10.1016/j.jsc.2020.09.003
- 739 12. Karcher MD, Carvalho LM, Suchard MA, Dudas G, Minin VN (2020) Estimating effective
740 population size changes from preferentially sampled genetic sequences. *PLoS Comput*
741 *Biol* 16(10): e1007774. <https://doi.org/10.1371/journal.pcbi.1007774>
- 742 13. Vavilova, V., Konopatskaia, I., Blinov, A. et al. Genetic variability of spelt factor gene in
743 *Triticum* and *Aegilops* species. *BMC Plant Biol* 20, 310 (2020).
744 <https://doi.org/10.1186/s12870-020-02536-8>
- 745 14. Chong, E.T.J., Neoh, J.W.F., Lau, T.Y. et al. Genetic diversity of circumsporozoite protein in
746 *Plasmodium knowlesi* isolates from Malaysian Borneo and Peninsular Malaysia. *Malar J*
747 19, 377 (2020). <https://doi.org/10.1186/s12936-020-03451-x>
- 748 15. Maloney EM, ... , Esquivel CO, Martinez OM, "Genomic variations in EBNA3C of EBV
749 associate with posttransplant lymphoproliferative disorder", *JCI Insight*.
750 2020;5(6):e131644. <https://doi.org/10.1172/jci.insight.131644>.
- 751 16. Huelsenbeck JP, Larget B, Alfaro MR, Bayesian Phylogenetic Model Selection Using
752 Reversible Jump Markov Chain Monte Carlo, *Molecular Biology and Evolution*, Volume
753 21, Issue 6, June 2004, Pages 1123–1133, <https://doi.org/10.1093/molbev/msh123>
- 754 17. Wikipedia, Markov Chain, https://en.wikipedia.org/wiki/Markov_chain
- 755 18. Personal email communication, Kishony R.
- 756 19. Elixhauser A, Owens P. Reasons for Being Admitted to the Hospital through the

- 757 Emergency Department, 2003: Statistical Brief #2. 2006 Feb. In: Healthcare Cost and
758 Utilization Project (HCUP) Statistical Briefs [Internet]. Rockville (MD): Agency for
759 Healthcare Research and Quality (US); 2006 Feb-. Available from:
760 <https://www.ncbi.nlm.nih.gov/books/NBK63506/>
- 761 20. Agency for Healthcare Researcher and Quality, HCUP Fast Stats - Most Common
762 Diagnoses for Inpatient Stays, [https://www.hcup-](https://www.hcup-us.ahrq.gov/faststats/NationalDiagnosesServlet)
763 [us.ahrq.gov/faststats/NationalDiagnosesServlet](https://www.hcup-us.ahrq.gov/faststats/NationalDiagnosesServlet)
- 764 21. Friedman B, Henke RM, Wier LM. Most Expensive Hospitalizations, 2008: Statistical Brief
765 #97. 2010 Oct. In: Healthcare Cost and Utilization Project (HCUP) Statistical Briefs
766 [Internet]. Rockville (MD): Agency for Healthcare Research and Quality (US); 2006 Feb-.
767 Available from: <https://www.ncbi.nlm.nih.gov/books/NBK52654/>
- 768 22. Ventola CL. The antibiotic resistance crisis: part 1: causes and threats. P T. 2015
769 Apr;40(4):277-83. PMID: 25859123; PMCID: PMC4378521.
- 770 23. Llor, C., & Bjerrum, L. (2014). Antimicrobial resistance: risk associated with antibiotic
771 overuse and initiatives to reduce the problem. Therapeutic advances in drug safety, 5(6),
772 229-241. <https://doi.org/10.1177/2042098614554919>
- 773 24. Chang Y, Chusri S, Sangthong R, McNeil E, Hu J, Du W, Li D, Fan X, Zhou H,
774 Chongsuvivatwong V, Tang L. Clinical pattern of antibiotic overuse and misuse in
775 primary healthcare hospitals in the southwest of China. PLoS One. 2019 Jun
776 26;14(6):e0214779. doi: 10.1371/journal.pone.0214779. PMID: 31242185; PMCID:
777 PMC6594576.
- 778 25. Samantha, Difference Between HA-MRSA and CA-MRSA, Posted Nov. 22, 2017,
779 <https://www.differencebetween.com/difference-between-ha-mrsa-and-vs-ca-mrsa/>
- 780 26. Margolis E, Rosch JW. Fitness Landscape of the Immune Compromised Favors the
781 Emergence of Antibiotic Resistance. ACS Infect Dis. 2018 Sep 14;4(9):1275-1277. doi:
782 10.1021/acsinfecdis.8b00158. Epub 2018 Aug 2. PMID: 30070470; PMCID:
783 PMC6358436.
- 784